A COMPUTER SIMULATION OF USING A LARGE REFLECTOR ANTENNA FOR MICROWAVE HYPERTHERMIA

Hua-Cheng Chang and Kenneth K. Mei
Department of Electrical Engineering and Computer Sciences
and the Electronics Research Laboratory
University of California, Berkeley, CA 94720 U.S.A.

I. INTRODUCTION

The use of heat to cause elevated tumor temperature at 42°C or higher (hyperthermia) has received a great interest in recent years, since in general malignant cells are more sensitive to heat than normal cells in the range of 42-45°C [1]. In addition, most tumors have much less blood perfusion rate than their surrounding normal tissues have, meaning that they may be preferentially heated [2]. Thus, obtaining a localized tumor temperature has been an important task in hyperthermic therapy. However, for non-invasive treatment, it is still difficult to produce well controlled elevated temperature distributions (in the range of 42-45°C) in the tumor without overheating normal tissue. For examples, ultrasound has good localization and deep penetration into human muscle but its limitation comes from the high absorption in bone, causing bone heating. As for electromagnetic wave, people have been using divergent waves widely which often induce maximum heating on the tissue surface with an exponential decrease with depth. Although low frequency does give a good penetration, its poor focusing may still hurt the normal tissue [3]. By using a parabolic reflector to focus an electromagnetic pulse, this paper presents a way that can generate both good focusing and satisfactory penetration, meaning that an elevated tumor temperature can be obtained without overburning the surrounding normal tissue.

The approaches in this study contain the generation of focused electromagnetic pulse, the penetration of this pulse into a biological material, and the calculation of the temperature profile in the biological material. First, a plane wave of modulated Gaussian pulse is transmitted towards a three dimensional parabolic reflector, which causes a high intensity field around the focal point, as the wave passes. Next, this focusing field is directed towards a biological material, the time sequence of the penetration of the fields into the material can be observed. The above two tasks are completed by solving the Maxwell's equations with the point-matched time domain finite element method [4]. Afterwards, the temperature profile of the biological material can be calculated through the bio-heat transfer equation [5]. Furthermore, the localization properties of the temperature profile can be adjusted by varying the related parameters.

This research was supported by the Office of Naval Research Contract N00014-86-K-0420.

II. FORMULATION

The configuration of the generation of focused pulse is shown in Fig. 1 where a 3-D axially symmetric parabolic reflector is illuminated by an x-polarized plane wave of modulated Gaussian pulse. In order to find the focused fields, we solve the source-free Maxwell's equation:

$$\nabla\times\bar{E}(\bar{r},t) = -\mu_0\frac{\partial\bar{H}(\bar{r},t)}{\partial t} \tag{1}$$

$$\nabla\times\bar{H}(\bar{r},t) = \sigma\bar{E}(\bar{r},t) + \varepsilon\frac{\partial\bar{E}(\bar{r},t)}{\partial t} \tag{2}$$

where the unknowns are the electric field $\bar{E}$ and the magnetic field $\bar{H}$ which in this project represent the *scattered* fields. The conductivity σ and the permittivity ε take different values in their respective media for the inhomogeneity of the surrounding material of the reflector. By the finite element method, the $\bar{E}$ and $\bar{H}$ are discretized in the space $\bar{r}$. The fields within an element are represented as a linear combination of its nodes:

$$\bar{E}(\bar{r},t) \approx \sum_{l=1}^{4} \phi_l(\bar{r})\ \bar{E}_l(t) \tag{3}$$

$$\bar{H}(\bar{r},t) \approx \sum_{l=1}^{4} \psi_l(\bar{r})\ \bar{H}_l(t) \tag{4}$$

where ϕ_l's and ψ_l's are known basis functions. The finite element meshes are shown in Fig. 2. Substituting the above functional forms into (1) and (2) and equating both sides on nodes j at $\bar{r}_j$ for (1) and on nodes i at $\bar{r}_i$ for (2), we obtain:

$$-\mu_0\frac{\partial\bar{H}_j}{\partial t} = \sum_{l=1}^{4} \nabla\phi_l(\bar{r}_j)\times\bar{E}_l(t) \tag{5}$$

$$\sigma\bar{E}_i + \varepsilon\frac{\partial\bar{E}_i}{\partial t} = \sum_{l=1}^{4} \nabla\psi_l(\bar{r}_i)\times\bar{H}_l(t) \tag{6}$$

The intergration of (5) and (6) starting from the initial condition will give the transient response of the problem. Here the leap-frog scheme is incorporated where the two field quantities are defined on alternative half time step: $\bar{E}_i$'s are computed at temporal nodes t = nδt and $\bar{H}_j$'s at t = (n-½)δt, n = 0, 1, 2, ... We can then approximate the time derivatives in (5) and (6) by central difference formulas and can obtain the recurrence formulas:

$$\bar{H}_j^{\,n+½} = \bar{H}_j^{\,n-½} - \frac{\delta t}{\mu_0}\sum_{l=1}^{4} \nabla\phi_l(\bar{r}_j)\times\bar{E}_l^{\,n} \tag{7}$$

$$\bar{E}_j^{\,n+1} = \frac{2\varepsilon - \sigma\delta t}{2\varepsilon + \sigma\delta t}\ \bar{E}_j^{\,n} + \frac{2\delta t}{2\varepsilon + \sigma\delta t}\sum_{l=1}^{4} \nabla\psi_l(\bar{r}_i)\times\bar{H}_l^{\,n+½} \tag{8}$$

for the time integration of state equations. The initial condition being known, with suitable treatment of the conducting boundary and the truncation boundary, Eqs. (9) and (10) can be applied alternating for $\bar{H}_j^{\,n+½}$'s and $\bar{E}_i^{\,n+1}$'s with n = 0, 1, 2, ...

Since $\bar{E}(\bar{r},t)$ is obtained, through the bio-heat transfer equation, the initial temperature rise can be calculated by

$$\Delta T = \frac{1}{\rho_{ts} c_{ts}} \int \sigma_{ts} \left| \bar{E}(\bar{r},t) \right|^2 dt \qquad (9)$$

where $\Delta T = T(t=0^+) - 37°C$ is the initial temperature rise, ρ_{ts} is the tissue's density, c_{ts} is the specific heat, and σ_{ts} is the electric conductivity.

III. NUMERICAL RESULTS

The focused pulse by the reflector in Fig. 1 is presented in Fig. 3. Note that the peak value of the focused pulse is about 45 times larger than that of the incident pulse. Here the surrounding material around the reflector is purposely chosen as a mixture of fresh water and ethanol which makes the material relative permittivity be 49 and conductivity be 10^{-3} s/m.

With the presence of human muscle, the initial temperature distribution is obtained and penetration depth and the localization volume are also defined in this study. In Fig. 4, the human muscle is considered as a cylinder with surfaces at I = 0 and J = -6 and 6 cm, and outside the muscle is the same mentioned liquid mixture. This figure depicts that the penetration depth is 5 cm from the front surface and 6 cm from both side surfaces. The localization volume is defined as the volume enclosed by the equal temperature contour of 42°C, which is about 2 cm wide and 4 cm long in Fig. 4. The factors which may influence the properties of penetration and localization are also studied. Those factors include the applied frequency, the associated biological conductivity, and the size of the reflector. The localization is better, i.e. the localization volume is smaller, when the applied frequency is higher or the size of the reflector is bigger; the penetration is deeper if the biological electric conductivity is smaller.

IV. CONCLUSIONS

The generation of a localized temperature distribution inside the human muscle has been carried out numerically through the use of a parabolic reflector to focus an electromagnetic pulse. The temperature is localized so it can heat a specific spot without overburning the surrounding tissue. Also, the penetration depth and localization volume can be controlled by the adjustment of the applied frequency and the parameters of reflector. In addition, the advantage of the time domain finite element method is its simplicity in programming since no matrix is involved. However, at present the capacity of computer memory limits a more realistic model of human muscle.

An experiment to verify the simulation results is now under preparation. Additionally, a more practical model for human muscle needs to be established, meaning that more computer memory is needed in the future.

REFERENCES

[1] J. G. Short and P. F. Turner, "Physical hyperthermia and cancer therapy," *Proc. IEEE*, vol. 68, pp. 131-142, Jan. 1980.

[2] C. W. Song, A. Lokshina, J. G. Rhee, M. Patten, and S. H. Levitt, "Implication of blood flow in hyperthermic treatment of tumors," *IEEE Trans. Biomed. Eng.*, vol. BME-31, pp. 9-16, Jan. 1984.

[3] A. Y. Cheung and A. Neyzari, "Deep local hyperthermia for cancer therapy: external electromagnetic and ultrasound techniques," *Cancer Research (Suppl.)* 44, pp. 4736-4744, Oct. 1984.

[4] A. C. Cangellaris, C. C. Lin, and K. K. Mei, "Point-matched time domain finite element methods," National Radio Science Meeting, Boston, MA, June 1984.

[5] I. Chatterjee and O. P. Gandhi, "An inhomogeneous thermal block model of man for the electromagnetics environment," *IEEE Trans. Biomed. Eng.*, vol. BME-30, pp. 707-716, Nov. 1983.

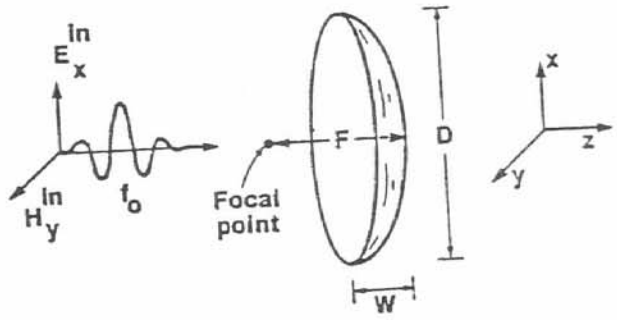

Fig. 1. Configuration of generation of focused pulse.
Diameter D = 144 cm
Depth W = 28.8 cm
Focal length F = 45 cm
Center frequency f_0 = 1 GHz

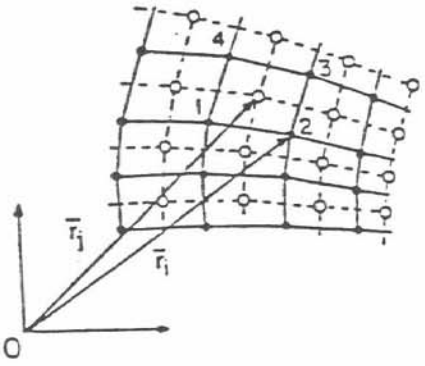

Fig. 2. Two complementary finite element meshes for the electric and magnetic fields.

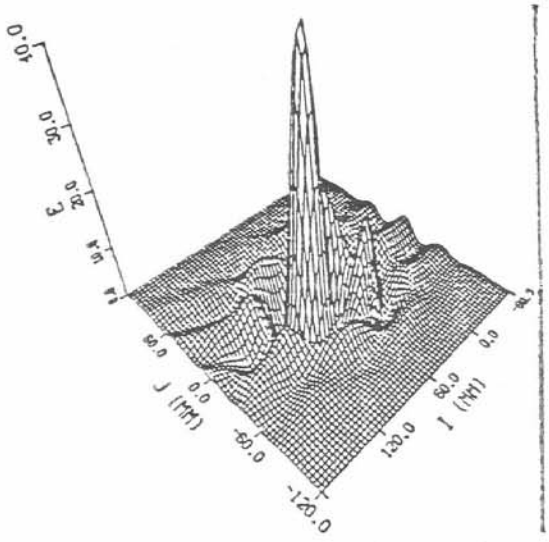

Fig. 3. Focused electric field in y-z plane around the focal point (I = 60 mm, J = 0 mm) with the absence of human muscle. Note that the peak value of the incident electric field is normalized to one.

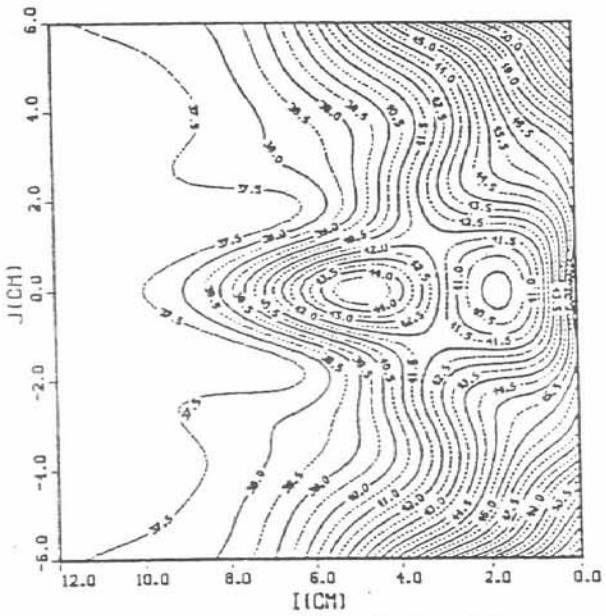

Fig. 4. Initial temperature distribution (°C) in y-z plane inside the human muscle. The muscle's surfaces are at I = 0 cm, and J = -6, 6 cm.